Earthquake Engineering. Tenth World Conference © 1992 Balkema, Rotterdam. ISBN 90 5410 060 5

Earthquake loading on R/C beam-column connections

G.S.Raffaelle, T.R.Gentry & J.K.Wight
University of Michigan, Ann Arbor, Mich., USA

ABSTRACT: Special R/C beam to column connections often found in framed structures have been tested under simulated earthquake loading at the University of Michigan Structural Engineering Laboratory. These connections include wide beam-column connections and eccentric beam-column connections. Wide beam-column connections were found to perform well if design parameters are carefully controlled. The major parameters which must be controlled are the beam-width to column-width ratio and the fraction of the total longitudinal steel anchored in the transverse beam. For exterior beam-column connections, if the spandrel beam width is less than the column width, the beam axes are eccentric to the column axis. The experimental program investigated the effect of varying the beam width, the beam depth, and the amount of longitudinal beam reinforcement on the behavior of the connection. From the test results, an equation for the effective joint width of eccentric connections is proposed.

1. SPECIAL CONNECTION TESTS

Wide beam-column connections, whose beams are wider than their supporting columns, are often found in one-way concrete joist systems and in other concrete buildings where floor-to-ceiling heights are restricted and congestion in the column core is expected. Wide beam-columns are currently prohibited in high seismic zones by ACI-ASCE Committee 352 (1985).

The other special case considered is eccentric beam-column connections. In this type of connection the beam width is less than the column width, and the beam axes are eccentric to the column axis. The experimental program investigates the effect of varying the beam width, the beam depth, and the amount of longitudinal beam reinforcing on the behavior of the connection.

1.1 *Experimental Setup*

Both the wide beam specimens and the eccentric beam specimens were tested by imposing a lateral displacement at the top of the column. The base of the column and the beam ends were pinned, consistent with the assumption that these locations were the inflection points for the lateral load moment diagram (see Fig. 1). Increasing story drifts from 0.5% to 5.0% were applied to the specimens. An axial load of 90 kN was applied to the column to preclude tension in the column during testing.

2. WIDE BEAM-COLUMN CONNECTIONS

Testing of wide beam-column connections stems from the recommendation by ACI-ASCE Committee 352 that these connections be experimentally evaluated for use in high seismic zones (1985). A major goal of the test program was to investigate the wide beam restrictions found in the ACI Code (1989),

$$b_w \leq b_c + 1.5h_w, \tag{1}$$

and in the New Zealand Code (1982),

$$b_w \leq b_c + h_c/2 \text{ and } b_w \leq 2b_c, \tag{2}$$

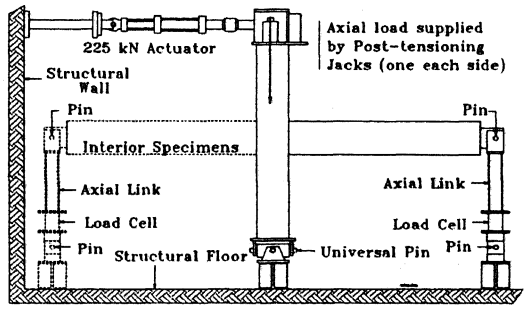

Figure 1. Testing frame for connection specimens.

Table 1. Wide beam-column connection specimen design parameters.

No.	b (mm)	b_w/b_c	Beam Longitudinal Reinforcement[1] Top	Bot.	M_r[2]	$\gamma = v_j/\sqrt{f'_c}$[3]	% Steel in Core Top	Bot.
1	864	2.43	9 #5	7 #5	1.50	1.26	33%	43%
2	762	2.14	8 #5	6 #5	1.69	1.12	50%	33%
3	864	2.43	2 #6, 2 #5, 6 #4	3 #5, 6 #4	1.49	1.23	56%	44%
4	864	2.43	10 #5, 2 #4	8 #5, 2 #4	1.18	1.60	35%	35%

Notes: 1: U.S. reinforcing bar sizes, 2: $M_r = \Sigma M_{n(\text{column})} / \Sigma M_{n(\text{beam})}$, 3: Calculated in MPa

where b_w is the width of the wide beam, b_c is the width of the column, h_w is the depth of the wide beam, and h_c is the depth of the column.

The wide beam-column experimental program consisted of the testing of four exterior 3/4-scale specimens, including transverse beam with reinforcement. The effects of joint shear stress level, amount of beam longitudinal reinforcement anchored in the transverse beam, and beam-width to column-width ratio (b_w/b_c) were explored as part of this experimental research. Information from interior wide beam testing performed in Japan (Hatamoto et al. 1991) supplemented the data from the testing performed at the University of Michigan. In addition to the experiments, computer simulation of R/C frames using wide beams was performed. The results from these analyses were compared to analyses of typical R/C frames.

Table 1 outlines the design parameters for the four specimens. All four specimens employed 356 mm square columns and 305 mm deep beams. Specimens 1, 3, and 4 exceeded the ACI maximum beam width of 813 mm from Eq. (1). All four specimens exceed the New Zealand maximum beam width of 533 mm from Eq. (2). All specimens violated the ACI-ASCE Committee 352 recommendations for column bar development in the connection. The specimens had a h(beam)/d_b(column) ratio of 16, less than the recommended value of 20.

2.1 *Summary of Wide Beam-Column Tests*

Results from the test of Specimen 1 (b_w/b_c = 2.43) indicated that torsional distress in the transverse beam, along with anchorage loss for the wide beam flexural reinforcement, were the primary causes of wide beam connection failure (see Fig. 2). This specimen's transverse beam did not have the capacity to transfer the torque applied by the wide beam to the column. Consequently, the bars anchored outside of the failure surface (see Fig. 2) did not yield during the test.

Specimen 3, which had the same design strength and b_w/b_c ratio as Specimen 1, performed well. By moving some of the wide beam reinforcement from the transverse beam into the column core, the torsional distress and anchorage loss seen in Specimen 1 was avoided. Full yield of all wide beam longitudinal bars occurred at 2.0% lateral drift. Figure 3 shows the story shear versus drift relationship for Specimens 1 and 3. The figure shows that Specimen 3 was stiffer, stronger, and able to dissipate more energy than Specimen 1.

The calculated cracking torque of the transverse beam was used to limit the amount of wide beam longitudinal steel anchored in the transverse beam of Specimen 3. This prevented the transverse beam from cracking in torsion.

Specimen 2 also performed well. The wide beam with a b_w/b_c ratio of 2.0 and the accompanying drop in torsional demand on the transverse beam (as compared to Specimen 1) eliminated the cracking of the transverse beam. Therefore all of the wide beam longitudinal steel yielded and retained its anchorage during the test.

Both the column core and the transverse beam of

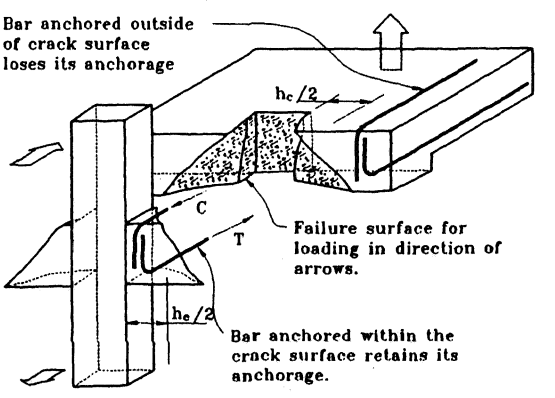

Figure 2. Typical exterior wide beam failure surface (after Durrani 1987).

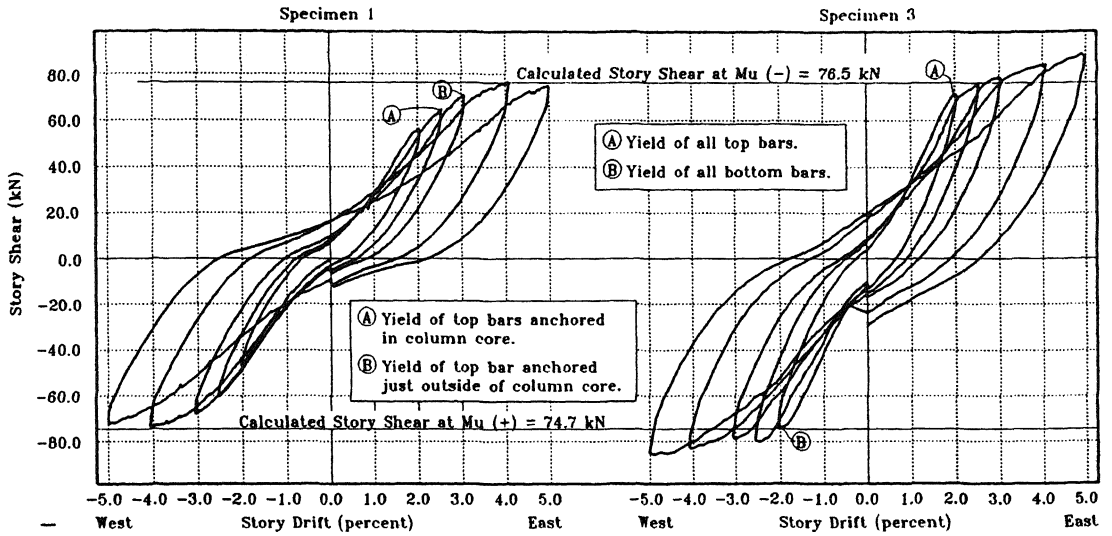

Figure 3. Story-shear versus displacement relationship for wide beam specimens 1 and 3.

Specimen 4 was heavily reinforced, thus this specimen did not perform well. The transverse beam failure (Fig. 2) kept the exterior wide beam bars from reaching yield.

Behavior of the wide beam plastic-hinging region: In Specimens 1 and 2 no flexural or shear distress of the wide beam plastic-hinging region was observed. Most cracks were vertical (i.e., flexural); no cracks arced over into flexural-shear cracks. In no location did top and bottom cracks join to form a failure plane through the wide beam. No spalling of cover concrete occurred in any of the specimens tested.

In Specimens 3 and 4, the spacing of the shear reinforcement in the plastic-hinging region was increased and the number of stirrup legs reduced from 6 to 4. Good behavior of the plastic-hinging region was still observed. The low shear stress on the cross-section of the wide beam was responsible for this lack of shear distress.

2.2 *Detailing Recommendations*

From the results of this research, the following detailing recommendations are suggested:

1. The limitation on the width of wide beams, found in the ACI Code (Eq. (1)), should be changed to

$$b_w \leq b_c + 2h_c, \qquad (3)$$

in conjunction with recommendation 2 below.

2. For exterior connections, the bars anchored in the transverse beam outside of a line $h_c/2$ from the face of the column (see Fig. 2) should not exert a torque greater than the cracking torque of the transverse beam. The cracking torque may be calculated using the formula presented by Hsu (1968):

$$T_{cr} = f_t \left[\frac{x^2 y}{3} \right] \qquad (4)$$

where f_t is the tensile strength of concrete and x and y are the dimensions of the transverse beam with $y \geq x$.

3. In exterior connections, the hooked bars anchored in the transverse beam should be placed so that the cover beyond the 90 degree hook is 50 mm or more. This will prevent the hooked bar from spalling the concrete on the exterior face of the transverse beam as it undergoes tension-compression cycling. Anchorage requirements for the hooked bar must still be met.

4. The maximum spacing of shear reinforcement and number-of-legs requirements for the beam plastic-hinging region (ACI Code, Section 21.3.3), should be relaxed for wide beams with low shear stress. The maximum spacing should be changed from $d/4$ to $3d/8$. The other spacing requirements (8 d_b on the longitudinal bar and 24 d_b on the stirrup) should remain unchanged. A confining stirrup leg should not be required for every other longitudinal bar (Section 21.3.3.3). Instead, a minimum of 4 stirrup legs should be used for the wide beam. These relaxed provisions should be used whenever the gross shear stress on the cross-section ($V_n/b_w d$) is below $0.17\sqrt{f'_c}$, where f'_c is the concrete strength in MPa.

5. The provision for column bars passing through passing through a joint, h(beam)/d_b(column) $\geq$ 20, should also be relaxed. Both these tests and test by Durrani and Zerbe (1987) show that good hysteretic behavior can occur even if the h(beam)/d_b(column) ratio falls as low as 16. The proposed value is h(beam)/d_b(column) $\geq$ 16.

Table 2. Eccentric beam-column connection specimen design parameters.

Specimen No.	Beam Size (mm)	Column Size (mm)	Eccentricity (mm)	Top Bars[1]	Bottom Bars[1]	Joint Shear Factor	Moment Strength Ratio
1	254x381	356x356	50.8	3-#6	3-#5	1.21	1.51
2	178x381	356x356	88.9	2-#6	2-#5	0.95	2.25
3	190x381	356x356	82.6	3-#5	2-#5	0.81	2.20
4	190x559	356x356	82.6	3-#5	2-#5	1.05	1.37

1: U.S. reinforcing bar sizes

3. ECCENTRIC BEAM-COLUMN CONNECTIONS

A related program investigated the behavior of reinforced concrete eccentric beam-column connections subjected to earthquake-type loading. The specimens represent a beam-column subassemblage from an exterior moment-resisting frame in which, for architectural purposes, the spandrel beams were made flush with the exterior face of the column. This type of eccentric connection is quite common yet is recognized by ACI-ASCE Committee 352 as an area of needed research (1985).

3.1 *Experimental Program*

All of the specimens had identical column sections and two beams framing into opposite sides of the column in such a way that the exterior face of the beam was flush with the column face. The major design parameters varied were the beam width, the beam depth, and the amount of top and bottom longitudinal reinforcing steel in the beam. By varying the beam width, the eccentricity between the column centerline and the beam centerline and the effective joint shear area also varies. The amount of reinforcing steel in the beam influences the horizontal shear demand on the joint and changes the beam-to-column moment strength ratio. The design parameters based on the actual material properties for the four specimens are given in Table 2. The following items are discussed as they relate to the adequacy of these eccentric type connections: hysteretic behavior and energy dissipation, deterioration of anchorage of longitudinal beam reinforcement, joint shear distortion, and joint shear strength.

3.2 *Test Results*

The load-displacement response of Specimen 1 to cyclic loading is shown in Fig. 4. The longitudinal beam reinforcement yielded between story drifts of 1.5 and 2%, and the strength of the specimen continued to increase as the cycles reached story drifts of 4%. The specimen, however, did not the reach the predicted strength of 112 kN which was determined by a nonlinear analysis. Diagonal cracking in the joint was more extensive on the outside face of the column than on the inside face. Torsional cracks on the sides of the column where the beams framed in were evident within the joint depth.

The load-displacement response of Specimen 2 is shown in Fig. 5. The maximum strength was reached at 3% story drift, and it was only 84% of the predicted

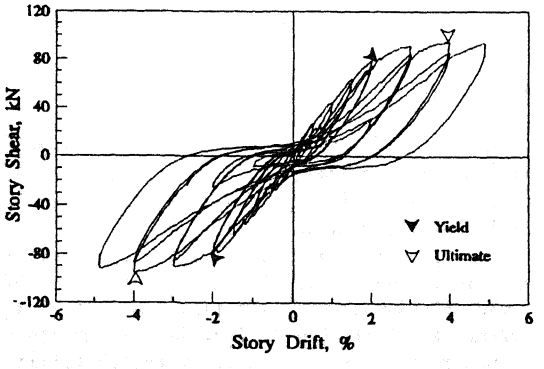

Figure 4. Load displacement response of eccentric Specimen 1.

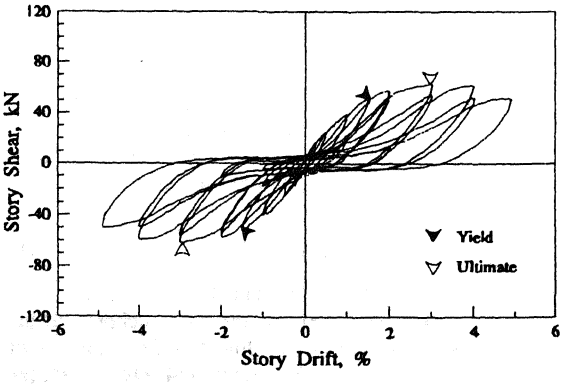

Figure 5. Load displacement response of eccentric Specimen 2.

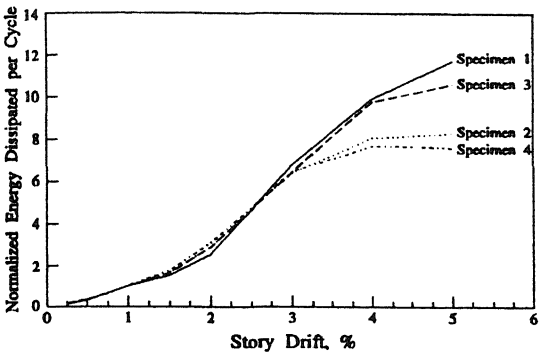

Figure 6. Normalized energy dissipated per cycle.

strength of 75 kN. The longitudinal beam bars began yielding between story drifts of 1.5% and 2%. The hysteresis loops for Specimen 2 show excessive pinching, and consequently small amounts of energy were dissipated. The pinching is primarily caused by the closing of cracks and the slippage of the beam bars through the joint. The development of diagonal cracking in the joint was similar to that of the first specimen. Torsional cracks in the column within the beam depth developed early in the loading sequence, but did not grow larger as the cycles progressed.

The load-displacement response of Specimens 3 and 4 also showed significant pinching. The behavior of the four specimens are compared in terms of the amounts of energy they were able to dissipate. For each specimen, the energy dissipated per cycle was normalized by the energy dissipated by that specimen during the first cycle to 1% story drift. Fig. 6 shows the normalized energy that was dissipated during cycles to increasing story drifts. The performance of the four specimens was similar up to 3% story drift. After 3%, Specimens 1 and 3 performed better than 2 and 4. Specimens 1 and 2 had the same size bars, but the improved performance of Specimen 1 is attributed to the larger beam width. Specimens 2 and 3 had approximately the same beam width, but smaller size bars were used in Specimen 3. The energy dissipating capability of Specimen 3 was greater than Specimen 2 because the smaller size bars improved the anchorage and decreased the pinching in the hysteresis loops. Specimens 3 and 4 had the same beam width and used the same size bars. The deeper beam in Specimen 4 caused the joint to deteriorate at a faster rate.

The measured strains in the reinforcement indicate that slippage of the beam bars did occur. The strains recorded in one of the top longitudinal beam bars at the beam-column interface for Specimen 1 and Specimen 2 are shown in Fig. 7 and Fig. 8, respectively. From simple beam theory it would be expected that the bar would be in compression for positive story drifts and in tension for negative story drifts. The strains in the figures for both specimens show that the bar is in tension for negative story drifts, but for positive story drifts the strain changes from the expected compression to tension as the percent story drift increases. The change from compression to tension indicates the anchorage of the beam bar in the joint has been partially lost. For Specimen 1, the bar did not go into tension until 2% story drift was reached and at 3% story drift the tensile strain was still very small. For Specimen 2, the bar was in tension after 0.5% story drift and reached a tensile strain of approximately one-half the yield value at 1.5% story drift. This indicates that the beam bars experienced more slippage in Specimen 2 than in Specimen 1. The slippage of the beam bars may be the predominate cause of the pinching in the hysteresis loops and the poor energy dissipation in the specimens.

In Fig. 9, the ratio of the maximum measured strength to the predicted strength is plotted versus the ratio of the maximum measured horizontal joint shear to the nominal joint shear for the four specimens. Also plotted are results from specimens tested in New Zealand (Lawrance et al. 1991) and Japan (Joh et al. 1991). The nominal joint shear was calculated as $1.0\sqrt{f'_c}$ (MPa) times the effective joint area. In all the specimens the imposed displacements were

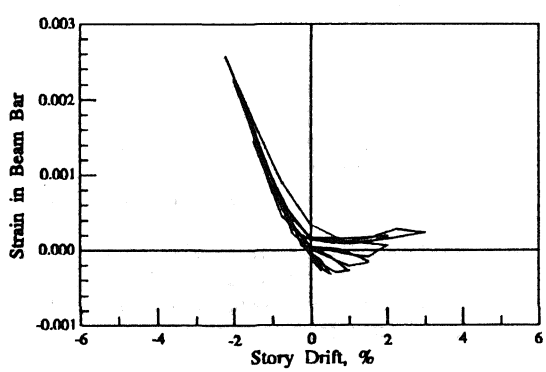

Figure 7. Strain in beam top longitudinal bar at column face in eccentric Specimen 1.

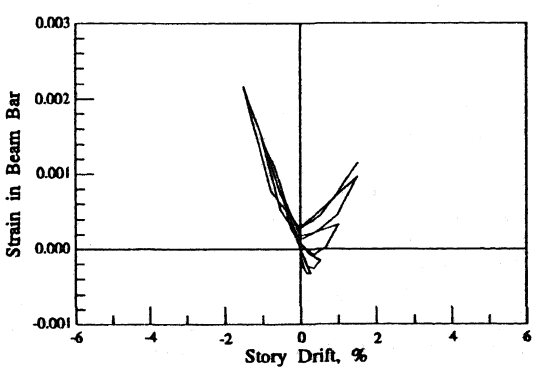

Figure 8. Strain in beam top longitudinal bar at column face in eccentric Specimen 2.

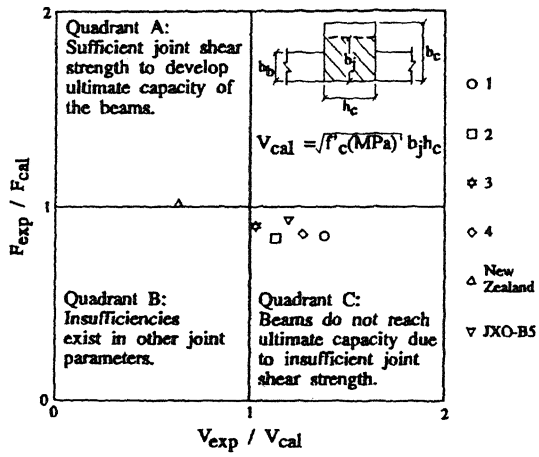

Figure 9. Interaction between applied load and horizontal joint shear based on the proposed equation for the effective joint width.

sufficient to reach the specimen's maximum strength. Neither plastic hinging in the columns nor yielding of joint hoops was observed in the specimens. Therefore, insufficient joint shear strength is the assumed reason for the specimens from this test not obtaining their predicted strength. The data points for all six specimens should therefore fall in either quadrant A or quadrant C of Fig. 9. Using the following equation for the effective joint width, the resulting scatter of data points was obtained:

$$b_j = \frac{b_c}{1+3e/x_c} \qquad (5)$$

where b_c is the column width, e is the joint eccentricity $= (b_c+b_b)/2$, and x_c is the smaller of b_c or h_c.

3.3 *Summary of Eccentric Beam-Column Tests*

The poor performance of the eccentric beam-column connections are primarily a result of the longitudinal beam bars losing anchorage within the joint. The joints showed some torsional distress at the beginning of the reversed cyclic loading pattern, but this damage did not increase as the cycles progressed. The poor anchorage condition is a result of the beam bars passing through the side of the joint where most of the deformation and diagonal shear cracking are concentrated. An equation for the effective joint width is proposed to the limit the horizontal joint shear that may be applied to an eccentric connection.

ACKNOWLEDGEMENTS

Support for this research by the United States National Science Foundation is gratefully acknowledged. The results and conclusions expressed here are those of the authors and do not necessarily reflect the views of the sponsor. Information from Hitoshi Hatamoto at the Kajima Construction Corporation in Japan, along with his colleagues Satoshi Bessho at Kajima and Prof. Yasuhiro Matsuzaki at the Tokyo Science University, is also gratefully acknowledged.

REFERENCES

ACI-ASCE Committee 352 1985. Recommendations for Design of Beam-Column Joints in Monolithic Reinforced Concrete Structures. *ACI Structural Journal* 82,3:266-283.

ACI Committee 318 1989. *Building Code Requirements for Reinforced Concrete* (ACI 318-89). Detroit, Michigan: American Concrete Institute.

Code of Practice for the Design of Concrete Structures (NZS 3101:1982) 1982. Wellington, New Zealand: Standards Association of New Zealand.

Durrani, A.J. and Zerbe, H.E. 1987. Seismic Resistance of R/C Exterior Connections with Floor Slab. *Journal of Structural Engineering.* ASCE. 113:1850-1864.

Hatamoto, H., Bessho, S., and Matsuzaki, Y. 1991. Reinforced Concrete Wide-Beam-to-Column Subassemblages Subjected to Lateral Load. *Design of Beam-Column Joints for Seismic Resistance* (ACI Publication SP-123). Detroit, Michigan: American Concrete Institute.

Hsu, T.T.C. 1968. Torsion of Structural Concrete-Behavior of Reinforced Concrete Rectangular Members. *Torsion of Structural Concrete* (ACI Publication SP-18). Detroit, Michigan: American Concrete Institute.

Joh, O., Goto, Y., and Shibata, T. 1991. Behavior of Reinforced Concrete Beam-Column Joints with Eccentricity. *Design of Beam-Column Joints for Seismic Resistance* (ACI Publication SP-123). Detroit, Michigan: American Concrete Institute.

Lawrance, G.M., Beattie, G.J., and Jacks, D.H. 1991. The Cyclic Load Performance of an Eccentric Beam-Column Joint. *Central Laboratories Report 91-25126,* New Zealand.